Journal of Enzyme Inhibition and Medicinal Chemistry

http://informahealthcare.com/enz
ISSN: 1475-6366 (print), 1475-6374 (electronic)

J Enzyme Inhib Med Chem, Early Online: 1–10
 DOI: 10.3109/14756366.2015.1014475

informa
healthcare

RESEARCH ARTICLE

Pyrazolo[1,5-a]quinazoline scaffold as 5-deaza analogue of pyrazolo[5,1-c][1,2,4]benzotriazine system: synthesis of new derivatives, biological activity on $GABA_A$ receptor subtype and molecular dynamic study

Gabriella Guerrini[1], Giovanna Ciciani[1], Samuele Ciattini[2], Letizia Crocetti[1], Simona Daniele[3], Claudia Martini[3], Fabrizio Melani[1], Claudia Vergelli[1], and Maria Paola Giovannoni[1]

[1]*Dipartimento NEUROFARBA, Sezione Farmaceutica e Nutraceutica, Università degli Studi di Firenze, Firenze, Italy,* [2]*Dipartimento di Chimica, Centro di Cristallografia, Università degli Studi di Firenze, Firenze, Italy, and* [3]*Dipartimento di Farmacia, Università degli Studi di Pisa, Pisa, Italy*

Abstract

To investigate the binding affinity of $GABA_A$ receptor subtype, new pyrazolo [1,5-a]quinazolines were designed, synthesized, and *in vitro* evaluated. These compounds, 5-deaza analogues of pyrazolo[5,1-c][1,2,4]benzotriazine derivatives which were already studied in our research group, permit us to evaluate the relevance of the nitrogen or the oxygen atom at 5-position of the tricyclic scaffold. Molecular dynamic study was done on a set of the new and known ligands to rationalize and to explain the lack of affinity on the 4- or 5-substituted new derivative. In fact, from biological results, it can be found that the only 5-unsubstituted new derivative, compound **15**, has receptor recognition ($K_i = 834.7$ nM).

Keywords

Fused tricyclic system, $GABA_A$ subtype receptor affinity, molecular modeling study, pyrazolobenzotriazine, pyrazoloquinazoline

History

Received 12 December 2014
Revised 22 January 2015
Accepted 22 January 2015
Published online 20 March 2015

Introduction

Fused tricyclic systems occur frequently in Medicinal Chemistry and are an attractive starting point for the design of ligands. Among the heteroatoms containing tricyclic rigid templates, the pyrazolo[5,1-c][1,2,4]benzotriazine represents a versatile system that let us to obtain selective subtype ligands to γ-aminobutyric acid type A receptor ($GABA_A$-R)[1,2]. In these compounds, we have reported a structure–activity relationship (SAR) and elaborated, in our laboratory, a ligand-based pharmacophoric model[3] to confirm the essential interaction points for the recognition of binding and the key-areas for modulation of the affinity. From these findings, we have obtained ligands with subnanomolar affinity as dual functional modulators (promnemonic and anxyolitic) and anthyperalgesic compounds on $GABA_A$-R[1,2].

As part of our lead optimization program, in the present work, we report the synthesize of new series of pyrazolo[1,5-a] quinazolines (A) as 5-deaza-analogues of the pyrazolo[5,1-c] [1,2,4]benzotriazine system (B), Scheme 1.

Compounds containing scaffold A are reported in the recent literature as negative allosteric modulators of metabotropic glutamate receptors 2 and 3 (dual mGlu2/mGlu3 NAMs)[4] and as non-camptothecin Topoisomerase 1 (Top1) inhibitors[5], while they have never been studied earlier as $GABA_A$ receptor ligands. Only tricyclic systems, containing pyrazole, triazole, and imidazole rings, which are condensed differently with quinoxaline, quinazoline and ftalazine, are reported for this study[6–9].

Thus, we synthesized the pyrazolo [1,5-a]quinazoline derivatives 3 and/or 4 and/or 5 which were substituted to enhance our SAR knowledge; moreover, a molecular dynamic study (MDS) and a principal component analysis (PCA) were performed to evaluate the requirements of $GABA_A$ receptor in the interaction with the ligands.

Materials and methods

Melting points were determined in open capillary tubes on a Büchi apparatus (Sigma, St. Louis, MO) and were uncorrected. IR spectra were recorded (in KBr pellets in nujol mulls) on Perkin-Elmer 1420 spectrophotometer (Perkin-Elmer, Waltham, MA). ^{1}H-NMR spectra were recorded with an Advance 400 Instrument (Bruker BiospinVersion 002 with SGU, Bruker AXS Inc., Madison, WI). Chemical shifts are reported in δ ppm using the solvent as an internal standard. Extracted samples were dried over Na_2SO_4 and the solvent was removed under reduced pressure. Merk F-254 commercial plates (Merk-Gruppe, Darmstadt, Germany) were used for analytical thin layer chromatography (TLC) to follow the reaction course. Silica gel 60 (70–230 mesh, Merck, Darmstadt, Germany) was used for column

Address for correspondence: Gabriella Guerrini, Dipartimento NEUROFARBA, Sezione Farmaceutica e Nutraceutica, Università degli Studi di Firenze, Via Ugo Schiff 6, 50019 Sesto Fiorentino, Firenze, Italy. E-mail: gabriella.guerrini@unifi.it

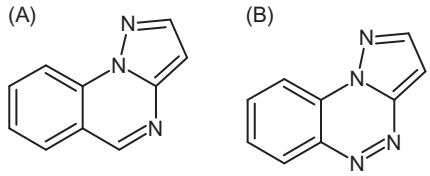

Scheme 1. Pyrazolo[1,5-a]quinazoline (A) and pyrazolo[5,1-c][1,2,4]benzotriazine (B).

chromatography. Microanalyses were performed with a Perkin-Elmer elemental analyzer (Perkin-Elmer, Waltham, MA) for C, H, and N. Results within ±0.4% of the theoretical materials were commercially available. Experimental data of more representative compounds are reported.

Chemistry

*3-Iodopyrazolo[1,5-a]quinazolin-5(4H)-one (**1c**)*

A solution of **1b** (0.050 g, 0.27 mmol) in dichloromethane (5 mL) was added to 0.40 mmol of iodine monochloride. The suspension was refluxed for 1 h and monitored by TLC. The final suspension was filtered and the precipitate was recovered. Cream crystals; yield 87%; TLC eluent: toluene/ethyl acetate/acetic acid 8:2:1 v/v/v. ^{1}H-NMR (DMSO): δ 12.26 (bs, 1H, NH exchange), 8.15 (d, 1H, H-9), 8.07 (d, 1H, H-6), 7.90 (t, 1H, H-7), 7.86 (s, 1H, H-2), 7.51 (t, 1H, H-8). IR cm^{-1}: 3228 (NH), 1678 (C=O). Anal Calcd for $C_{10}H_6IN_3O$: C 38.61; H 1.94; N 16.51. Found: C 38.48; H 1.79; N 16.39.

*General procedure for the synthesis of compounds **2a–c** and **2e***

To promote the deprotonation, the suitable starting material (**1a–c** and **1e**) and tBuOK (0.76 mmoles) were suspended in anhydrous DMF (5 mL) and stirred for 1 h at room temperature; then benzyl chloride (0.57 mmoles) was added and the mixture was refluxed for 2 h. The reaction was monitored by TLC (toluene/ethyl acetate/acetic acid 8:2:1 v/v/v as eluent) until the disappearance of the starting material. After cooling and addition of water, the formed precipitate was filtered and recrystallized by a suitable solvent.

*Ethyl 4-benzylpyrazolo[1,5-a]quinazolin-5(4H)-one-3-carboxylate (**2a**)*

Cream crystals; yield: 89%. ^{1}H-NMR (DMSO): 8.21 (s, 1H, H-2), 8.18 (m, 2H, H-9, H-6), 7.96 (t, 1H, H-7), 7.60 (t, 1H, H-8), 7.23 (m, 3H, H-3, H-4, and H-5 benzyl), 7.08 (d, 2H, H-2, and H-6 benzyl), 5.88 (s, 2H, CH_2), 4.11 (q, 2H, CH_2), 1.43 (t, 3H, CH_3). IR cm^{-1}: 1707, 1684 (CO). Anal Calcd for $C_{20}H_{17}N_3O_3$: C 69.15; H 4.93; N 12.10. Found: C 69.27; H 4.97; N 12.21.

*General procedure for the synthesis of compounds **4–6***

To the crude tosyl derivate (**1a′, 1c′** and **1d′**) in anhydrous DMF (3.0 mL), 0.6 mmoles of benzyl alcohol and 0.6 mmoles of tBuOK were added and the reaction was maintained at reflux temperature for 3 h. After cooling, water was added to the solution and the precipitate was filtered and purified by recrystallization. Compound **4** was obtained using either the corresponding 5-tosyl- or 5-chloro derivatives as the starting material. The two methods of synthesis are reported below.

*Ethyl 5-benzyloxypyrazolo[1,5-a]quinazoline 3-carboxylate (**4**)*

The title compound was obtained either from tosyl derivative (**1a′**) following the above mentioned method, yield 90%, or from 5-chloro derivative (**3**) but in low yield (35%). The followed procedure is reported: a solution of benzylic alcohol (0.21 mmoles) and tBuOK (0.21 mmoles) in anhydrous DMF (3.0 mL) was stirred for 1 h to permit the formation of the benzyloxy anion. Then, 0.14 mmoles were added to compound **3** and the reaction was refluxed for 2 h. After cooling, the addition of water gave a precipitate that was filtered and then the precipitate was recrystallized by methoxyethanol.

Cream crystals: TLC eluent: toluene/ethyl acetate/acetic acid 8:2:1 v/v/v. ^{1}H-NMR (DMSO-d_6): δ 8.44 (s, 1H, H-2), 8.36 (d, 1H, H-9), 8.23 (d, 1H, H-6), 8.07 (t, 1H, H-7), 7.69 (m, 3H, H-8, H-2′ and H-6′ phenyl), 7.42 (m, 3H, H-3′, H-4′ and H-5′ phenyl), 5.73 (s, 2H, CH_2), 4.32 (q, 2H, CH_2), 1.36 (t, 3H, CH_3). IR cm^{-1}: 1704 (COO). Anal Calcd for $C_{20}H_{17}N_3O_3$: C 69.15; H 4.93; N 12.10. Found: C 69.32; H 4.82; N 13.21.

*Ethyl 4,5-dihydropyrazolo[1,5-a]quinazoline-3-carboxylate (**14**)*

To a suspension of compound **3** (0.300 mmol) in 3.5 mL of THF anhydrous, 25 mg of Pd/C 10%, 1.0 mmol of ammonium formate, and 10 mL of methanol were added. The reaction was maintained at reflux temperature, and it was monitored by TLC (toluene/ethyl acetate/methanol 8:2:1.5 v/v as eluent), and after 2.5 h the starting material disappeared. The filtration of catalyst and the next evaporation of the solution gave a residue that was recovered by *i*-propyl ether. Off-white crystals: yield: 52%. ^{1}H-NMR (DMSO): δ 7.71 (d, 1H, H-2), 7.55 (d, 1H, H-9), 7.36 (t, 1H, H-8), 7.22 (d, 1H, H-6), 7.20 (bs, 1H, NH exchange), 7.19 (t, 1H, H-7), 4.53 (s, 2H, CH_2NH); 4.19 (q, 2H, CH_2); 1.26 (t, 3H, CH_3). IR cm^{-1}: 3337 (NH), 1692 (C=O). Anal Calcd for $C_{13}H_{13}N_3O_2$: C 64.19; H 5.39; N 17.27. Found: C 64.36; H 5.27; N 17.31.

*Ethyl pyrazolo[1,5-a]quinazoline-3-carboxylate (**15**)*

An excess of Pd/C (10%, 100 mg) was added to a solution of compound **14** (0.350 mmol) in 5 mL of toluene. The mixture was refluxed for 1 h followed by the filtration of catalyst and the solvent was evaporated. A yellow residue, recovered by *i*-propyl ether, was obtained. Yield: 50%. ^{1}H-NMR ($CDCl_3$): δ 9.21 (s, 1H, H-5); 8.55 (m, 2H, H-2, and H-9), 8.07 (d, 1H, H-6), 8.01 (t, 1H, H-8), 7.67 (t, 1H, H-7), 4.49 (q, 2H, CH_2); 1.46 (t, 3H, CH_3). IR cm^{-1}: 1692 (C=O). *Anal*. Calc. for $C_{13}H_{11}N_3O_2$: C 64.72; H 4.60; N 17.42. Found: C 64.59; H 4.69; N 17.31.

Radioligand binding assay

[^{3}H]Ro15-1788 (specific activity of 78.8 Ci/mmol) was obtained from Perkin-Elmer (Waltham, MA). All other chemicals were of reagent grade and were obtained from commercial suppliers. Bovine cerebral cortex membranes were prepared as previously described. The membrane preparations were diluted with 50 mM Tris-citrate buffer pH 7.4, and used in the binding assay. Protein concentration was assayed using the method of Lowry. [^{3}H]Ro 15-1788 binding studies were performed as previously reported[10]. At least six different concentrations of each compound were used. The data of $n = 5$ experiments carried out in triplicate were analyzed by means of an iterative curve-fitting procedure (program Prism, GraphPad, San Diego, CA), which provided IC_{50}, K_i, and SEM values for the tested compounds, the K_i values were calculated from the Cheng and Prusoff equation.

Docking calculation

The poses of ligands within the interaction site were searched with AUTODOCK[11] and only the amino acids that are in a range of 15 Å from the center of interaction site in the α/γ interface are considered to simplify the calculation.

The search area of poses, established by autogrid, was delineated by a cubic grid of 40 points (with a distance of

0.375 Å) for each coordinate. The genetic algorithm LGA (Lamarckian Genetic Algorithm), implemented in AUTODOCK 4, was used to search most of the probable ligand poses. The principal conditions imposed by LGA are the following: 150 was the number of individuals in population; 250 000 was the maximum number of energy evaluations; 27 000 was the maximum number of generations, 100 was the search realized by LGA, and the 100 were obtained poses which are collected in clusters with a similarity of 2 rms. From clusters, three poses are picked up: two poses belonging to the most abundant cluster and to the cluster with the best docking energy, while the third belongs to cluster with the second better docking energy. These three poses and the selected amino acids (within a range of 15 Å) constitute the starting complex conformation to molecular dynamic simulation.

Molecular dynamics method

The structures of ligands were built using the Discovery Studio 3.5 Visualizer free program (http://accelrys.com). The ligands' partial atomic charges were derived by using AM1-BCC[12] implemented in the ANTECHAMBER suite[13]. Energy minimizations and molecular dynamic simulations (MD) were carried out by using the SANDER module of AMBER 9[14] with the GAFF[15] force field.

For the dynamic simulation in water with periodic boundary condition, initially the entire system was subjected to energy minimization in two stages to remove bad contacts between the complex and the solvent molecules. First, the water molecules were minimized by holding the peptide chains fixed with a harmonic constraint of strength 2.0 kcal/(mol Å^2). Second, the entire system was minimized without restriction. The first stage was performed using the steepest descent minimization of 500 steps followed by a conjugate gradient minimization of 1000 steps and the second stage was performed by using the steepest descent minimization of 1000 steps followed by a conjugate gradient minimization of 5000 steps.

To solvate the part of interaction site released by the ligand, the system was soaked in a truncated octahedral periodic box of TIP3P[16] water molecules. The distance between the edges of the water box and the closest atom of the solutes was at least 2 Å.

The system was then heated from 0 to 300 K in 5 ps and equilibrated at 300 K for another 5 ps by holding the peptide chains fixed with a harmonic constraint of a strength of 2.0 kcal/(mol Å^2). After the minimization and heating, 100 ps of dynamic simulations by holding the peptide chains weakly fixed with a harmonic constraint of a strength of 0.01 kcal/(mol Å^2) were performed at a constant temperature of 300 K and a constant pressure of 1 atm.

During the minimization and MD simulations, the particle mesh Ewald method[17] was employed to treat the long-range electrostatic interactions in a periodic boundary condition. The Langevin dynamics with a collision frequency of 1.0 ps^{-1} was applied to control the temperature of the system. The SHAKE method[18] was used to constrain hydrogen atoms. The time step for all MD simulations was 2 fs, with a direct-space, non-bonded cutoff of 9 Å. Initial velocities were assigned from a Maxwellian distribution at the initial temperature.

In this study, the binding free energies were calculated by using the MM-PBSA method as implemented in the AMBER package. 100 snapshots were extracted from the MD simulation, and the binding free energies were calculated between the guest and the CD. The average binding free energies were calculated for every five snapshot getting 20 values of energy for MD trajectory.

In general, the binding free energies in the condensed phase can be calculated according to the following equations.

$$\Delta G_{\text{bind}} = G_{\text{complex}} - \left(G_{\text{ligand}} + G_{\text{peptide chains}}\right)$$
$$G = E_{\text{gas}} + G_{\text{solve}} - \text{TS}$$
$$E_{\text{gas}} = E_{\text{bond}} + E_{\text{angle}} + E_{\text{torsion}} + E_{\text{vdW}} + E_{\text{ele}}$$
$$G_{\text{solve}} = G_{\text{PB}} + G_{\text{SASA}}$$

where G_{complex}, G_{ligand}, and $G_{\text{peptide chains}}$ are the free energies of the complex, the molecule, and the CD, respectively. E_{gas} is the standard force field energy that consists of strain energies (E_{bond}, E_{angle}, and E_{torsion}). The solvation free energy (G_{solve}) is further divided into a polar component (GPB) and a non-polar one (GSASA). The polar component was calculated by using the PBSA program in AMBER 9.0[14], and in this work, the dielectric constant was set to 1 in solute and 80 in solvent. The non-polar component was determined by $\Delta G_{\text{nonpol}} = \gamma\text{SASA} + \beta$, in which SASA is the solvent-accessible surface area determined with MOLSURF[19]. In our calculations, the values for γ and β were set to 0.0072 kcal/mol Å^2 and 0 kcal/mol, respectively. The contribution of entropy (TS) to binding free energies via normal mode analyses is not evaluated as they usually have large error bars and require long simulation times.

Statistical analysis

The histograms were performed with Microsoft Excel (vers. 2013). The PCA was analyzed with the Statgraphics software for Windows (SAS Inc., Cary, NC).

Results and discussion

Chemistry

All compounds described here are listed in Table S1 and the synthetic strategies are depicted in Chart S1. The synthesis of the pyrazolo[1,5-a]quinazoline system, in a first attempt and the condensation of the 4-substituted-5-aminopyrazole with salicylic aldehyde, a two-component condensation are considered. The easily available starting materials, 4-ethoxycarbonyl- or 4-ciano-5-aminopyrazole and salicylic aldehyde, were reacted in dehydrating conditions using a Dean–Stark apparatus. The intermediate Schiff base, rapidly formed, would have to cyclize giving the desired pyrazolo[1,5-a]quinazoline nucleus through a synthetic strategy already used in our laboratory to synthesize the pyrazolo[5,1-c][1,2,4]benzotriazine derivatives[20]. In contrast, using other dehydrating methods (sublimation, high-boiling solvent), the reaction did not give good results and the aldimmine intermediate (base Schiff) was always recovered. Therefore, the synthesis of pyrazolo[1,5-a]quinazoline compounds was obtained starting from the well-known pyrazolo[1,5-a]quinazoline-5(4H)-one derivatives **1a–b** and **1d–e** (Table S1) and these derivatives were synthesized following reported methods[21–24]. The new 3-iodiopyrazolo[1,5-a]quinazoline-5(4H)-one, **1c,** was obtained by reacting **1b** with *N*-iodiosuccinimide (NIS).

In an attempt to synthesize the 5-benzyloxy derivatives, starting products (**1a–c** and **1e**) were reacted in anhydrous DMF, K_2CO_3, and benzyl chloride following a reported method for analogue compounds[25]. Unexpectedly, the reaction gave always the 4-*N*-benzyl derivatives (**2a, 2b,** and **2e**), even using different bases such as NaH and *t*-BuOK. Only starting compound **1c** gave a mixture of the two regio-isomers 4-*N*-benzyl- (**2c**) and 5-*O*-benzyl derivative (**5**) in a 1:1 ratio. This fact is probably due to a major steric hindrance of iodine atom in the 3-position that addressed the alkylation also in position 5 (Scheme 2). On the regioisomer **2a,** a crystallographic analysis was performed to confirm the structure (Figure S1).

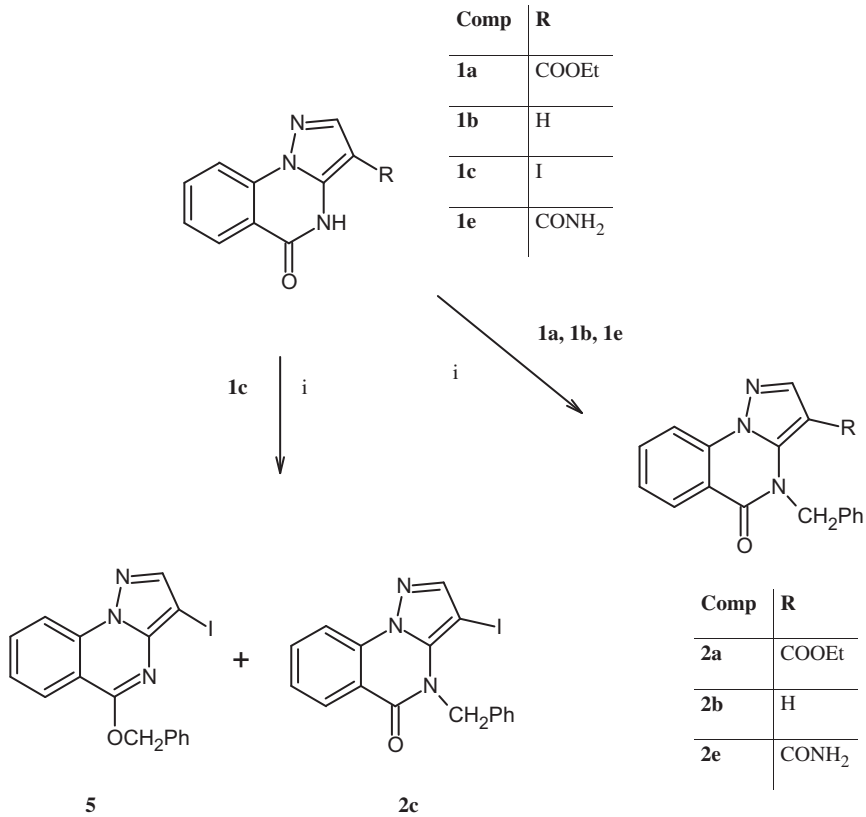

Scheme 2. Reagent and conditions: (i) DMF, K_2CO_3, benzyl chloride (for **1c**, a mixture of **2c** and **5** were obtained).

To obtain the desired benzyloxy derivatives, it was necessary to insert a suitable leaving group like a chlorine or a tosyl group at C-5 position of the pyrazolo[1,5-a]quinazoline system. The desired tosyl derivatives (**1a′, 1c′**, and **1d′**) were obtained in good yield and pure enough for the next reaction by the simple treatment of the lactam (**1a, 1c,** and **1d**) with tosyl chloride in DCM, in the presence of NEt_3. These intermediates were reacted in anhydrous DMF, *t*-BuOK, and benzyl alcohol to give the desired 5-benzyloxyderivatives (**4**–**6**).

When the starting materials **1a, 1c,** and **1d** were treated with $POCl_3$ to obtain the 5-chloroderivatives, only the ethyl 5-chloropyrazolo[1,5-a]quinazoline-3-carboxylate[26] **3** was recovered with good yield. Compound **3** was used to obtain the 5-aryl(heteroaryl)methylamino derivatives (**7**–**12**) by treating with an excess amount of suitable amine in DMF, as depicted in Scheme 3. To evaluate the relevance of hydrogen bond interaction with receptor protein in molecular dynamic study, compound **7** was hydrolyzed with the corresponding 3-carboxylic acid (**13**).

Finally, the 5-unsubstituted 3-ethoxycarbonylpyrazolo[1,5-a]quinazoline (**15**) was obtain starting from compound **3** by reduction with ammonium formate, 10% Pd/C in ethanol. Unexpectedly, the reduction gave the 4,5-dihydro derivative (**14**) and it was not possible to stop the reaction at the first step of reduction (5-H derivative) as reported in the literature[27]. Thus, the 4,5-dihydro derivative (**14**) was dehydrogenated to the desired compound (**15**) by an excess amount of 10% Pd/C in toluene at refluxed temperature (Scheme 4).

Experimental binding and molecular dynamic study

The Bz site/$GABA_A$-R binding affinity of newly synthesized compounds was evaluated by their ability to displace [^{3}H]flumazenil (Ro15-1788) from its specific binding in bovine brain membrane and was expressed as K_i value only for those compounds which inhibit radioligand binding by more than 80% at fixed concentrations of 10 μM. Unexpectedly, the arylalkylation at position 4- or 5- gave compounds that were unable to inhibit radioligand binding, while the only derivative that shows binding affinity in a nanomolar range was the ethyl pyrazolo[1,5-a]quinazoline 3-carboxylate (**15**) with $K_i = 834.7$ nM.

To explain that our compounds were not able to bind with the receptor protein, a molecular dynamic study and a PCA were performed using, as ''positive control'', some literature compounds: pyrazolo[5,1-c]quinazolines[6], 1,2,4-triazolo[1,5-a]quinoxalines[7], triazoloquinazolindiones[9], triazolo[1,5-a]quinazolines[8], imidazo[2,1-a]phtalazines[28], and triazolo[3,4-a]phtalazines[29].

To achieve our aim, compounds **1a**, **1b**, **1d**, **6**, **7**, and **13** and the positive references (**16**–**21**) were docked in a $hGABA_A$ receptor protein model, obtained by homology-modelling from acetylcholine-binding protein (AChBP)[30]. Since the ''benzodiazepine binding site'', or better said $GABA_A$ subtype receptor, is located between the alpha and the gamma subunits, the amino acids considered in this study belong to these two subunits. Compounds were grouped based on good affinity value (**16**–**18**, K_i range 0.62–74 nM), low affinity value (**19**–**21**, K_i range 243–570 nM), and inactive (**1a**, **1b**, **1d**, **6**, **7,** and **13**), Scheme 5.

In particular, the occurrence of hydrogen bonds and Van der Walls interactions between the ligand and the amino acids of receptor protein was evaluated. The ligand–receptor binding energy was calculated by AMBER 9[14] on three ligand–receptor complex conformations that were selected by AUTODOCK[11]. On the complex conformation that showed the better docking energy, the occurrence of hydrogen bonds and Van der Waals interactions between ligand and receptor protein was evaluated; the results of these interactions were plotted and the involved amino acids (of alpha1 and gamma subunits) stand out.

Scheme 3. (i) Tosylchloride, NEt_3, and DCM. (ii) DMF, t-BuOK, and benzyl alcohol. (iii) $POCl_3$, DIPEA. (iv) DMF and excess of suitable $Ar(Het)NH_2$. (v) Sodium hydroxide 10% solution, then HCl.

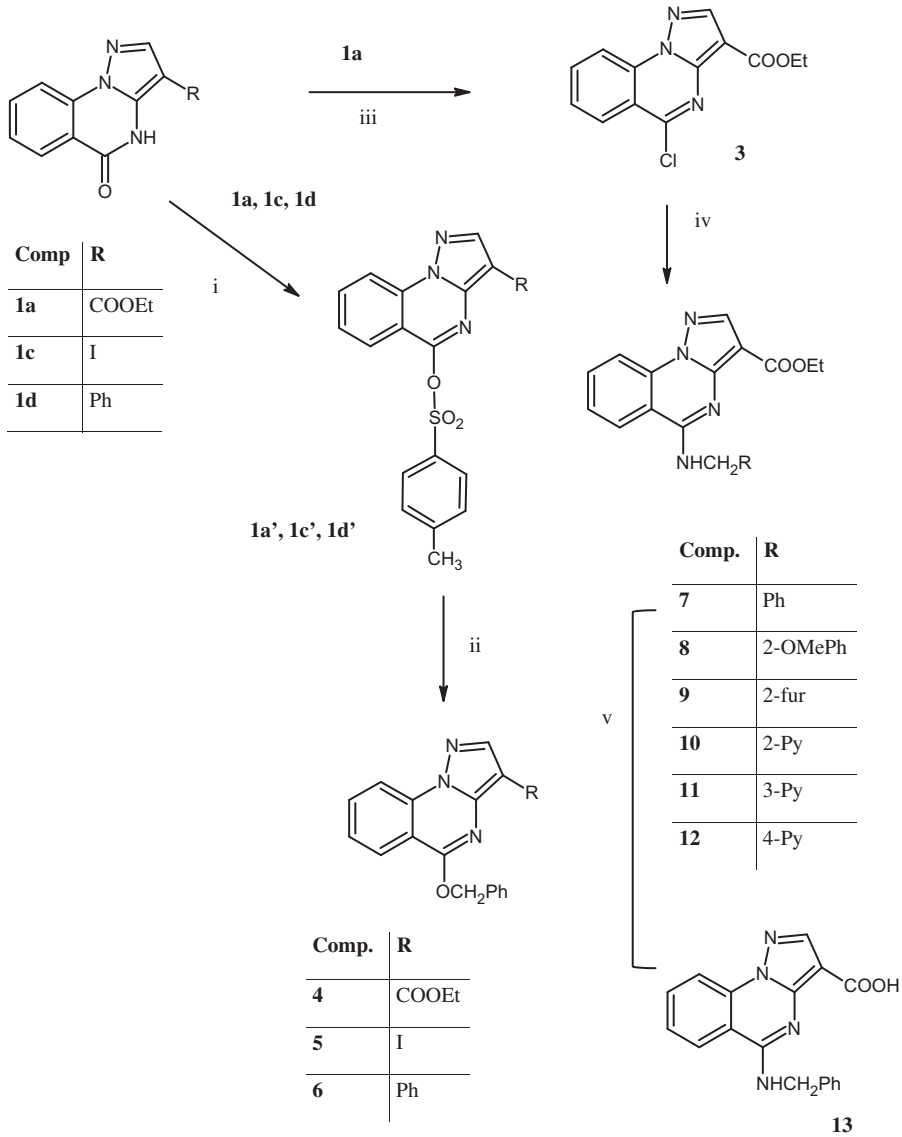

Comp	R
1a	COOEt
1c	I
1d	Ph

Comp.	R
4	COOEt
5	I
6	Ph

Comp.	R
7	Ph
8	2-OMePh
9	2-fur
10	2-Py
11	3-Py
12	4-Py

Scheme 4. Reagent and conditions: (i) EtOH, Pd/C 10%, and $HCOONH_4$; (ii) toluene and Pd/C 10% reflux.

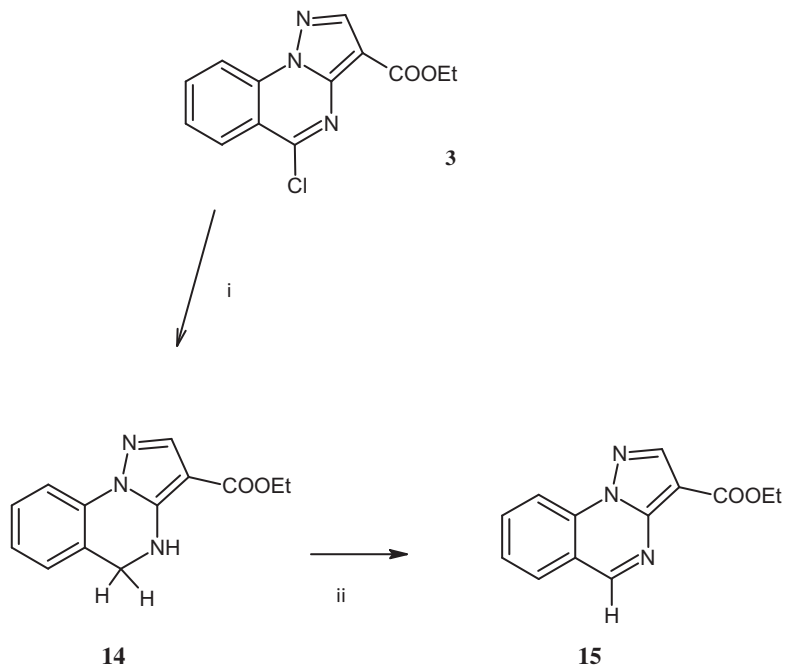

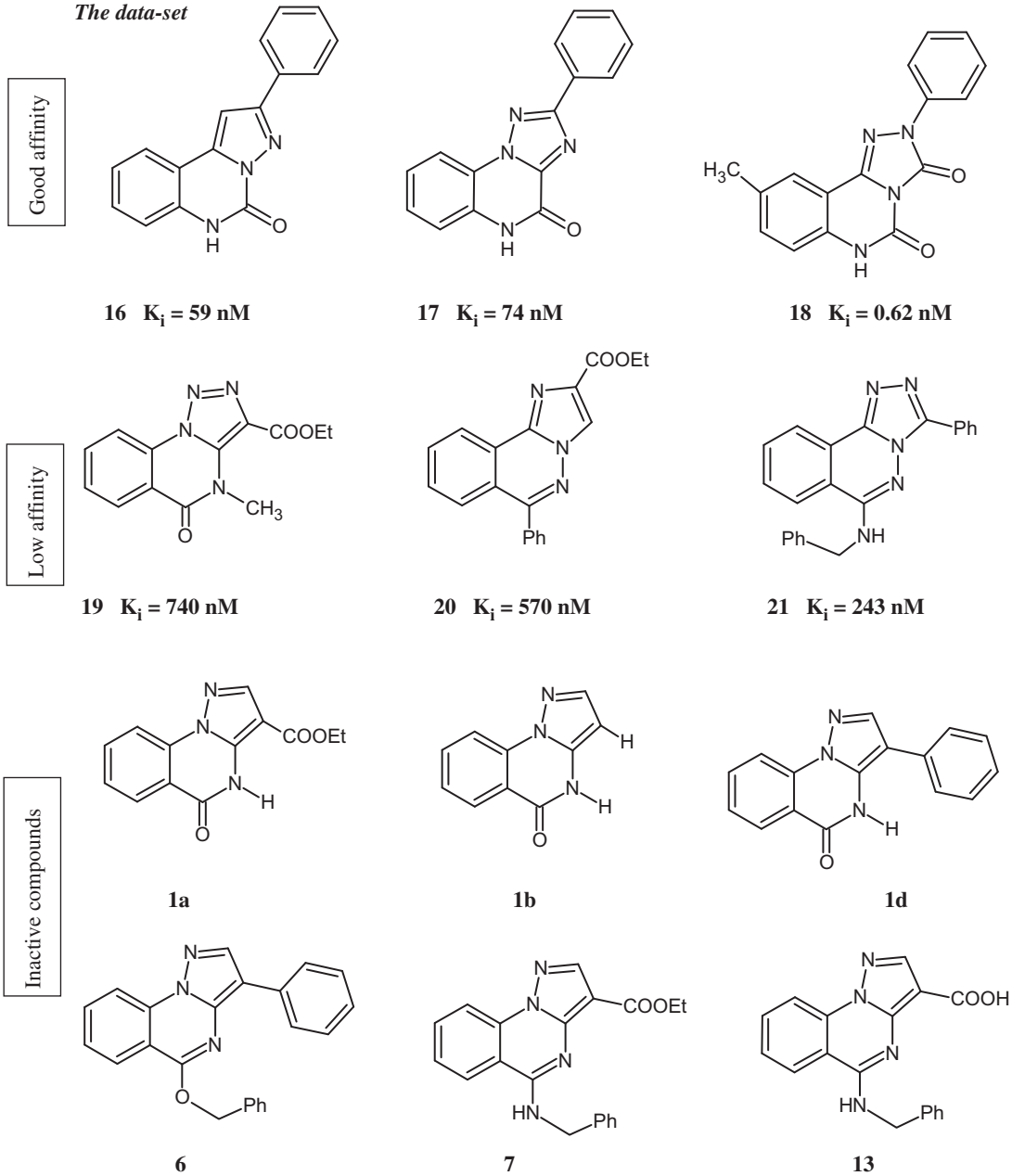

Scheme 5. The data-set.

In Figure 1(a) and (b), the histograms represent the average frequency of contacts (expressed in %) measured during the dynamic simulation of the ligand–receptor complex (hydrogen bond, Figure 1a and Van der Waals interactions, Figure 1b). The distribution of average occurrence of interactions is represented by black, grey, and white columns, respectively, for compounds with absent (**1a**, **1b**, **1d**, **6**, **7,** and **13**), low (**19–21**), and good affinity values (**16–18**). In particular, Figure 1(a) shows ligands which have major probability of hydrogen bond interactions in the following amino acids: the αY160 (Tyr 160), αS206 (Ser206), and γT142 (Thr142). The three ''families'' of ligands show different probabilities of the interaction with amino acids αY160 and γT142 unlike αS206 to be engaged, for which all ligands should have the same probability of hydrogen bond interaction. For Van der Waals interactions, the greater variation of interactions is evidenced with amino acids αA161 (Ala161), αV203 (Val203), αY210 (Tyr210), γM81 (Met81), and γY141 (Tyr141).

The frequencies of interaction with the alpha/gamma subunit amino acids that show greater changes have been used for PCA for the overall data set of 12 compounds, Figure 2. The first two principal components of the variables (% of frequencies contacts average) group together well enough the three types of ligands (inactive, black square; low affinity value, grey square; good affinity value, white square). From the PCA score's plot, it is observed that the most of the affine compounds (white square, **16–18**, K_i range 0.62–74 nM) engage hydrogen bond interaction through the NH proton, with an oxygen atom of γT142 carbonyl amidic group. For example, in Figure 3, the binding pocket and the relative orientation of ligand are depicted in compound **17**; hydrogen bond interaction, involving γT142, is represented by blue solid line. For the Van der Waals interaction, αV203 and αY210 are amino acids involved that engage hydrophobic interactions with the phenyl group at position 2 of compounds (pink dashed line) through the methyl groups and the phenyl ring.

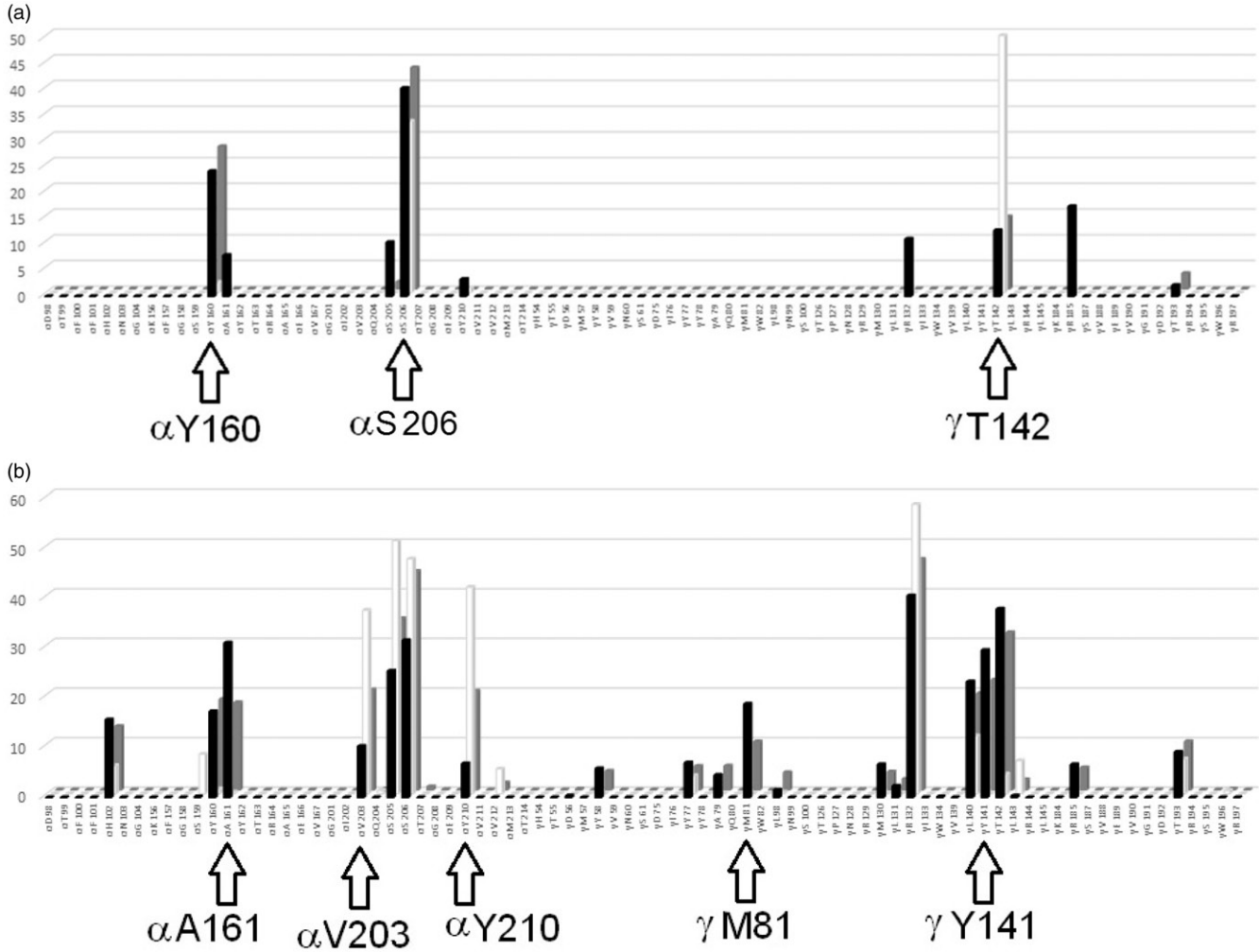

Figure 1. (a) Average frequency contacts (expressed in %) of hydrogen bond interaction measured during the dynamic simulation of ligand-receptor complex. White columns, affine ligands; grey columns, low affine ligands; black columns, inactive ligands. (b) Average frequency contacts (expressed in %) of Van der Waals interaction measured during the dynamic simulation of ligand–receptor complex. White columns, affine ligands; grey columns, low affine ligands; black columns, inactive ligands.

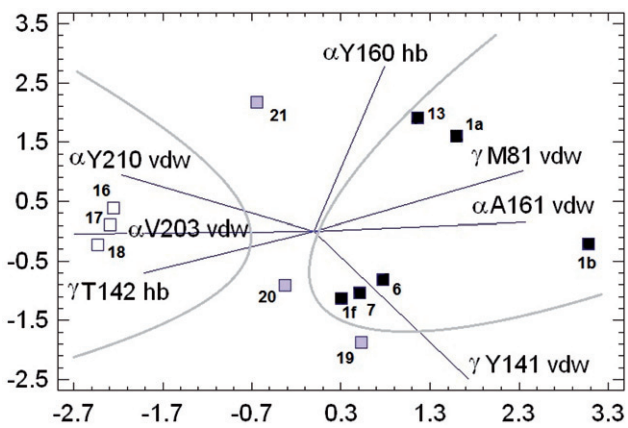

Figure 2. Principal components analysis. The ''biplot'' shows the value of the first two components of the original variables. The original variables considered are the average frequency (expressed in %) of hydrogen bonds (hb) and van der Waals (vdw) interactions between the ligand and the amino acids γT142, αY160, αY210, αV203, γM81, γY141, and αA161. The squares represent the ligands (white, affine; grey, low affine; black, inactive), the lines represent the component weights of the original variables.

The inactive compounds have low probability of interaction with γT142, αV203, and αY210 amino acids as they lack a hydrogen bond donor group (like NH) and a lipophilic group (like phenyl) at a proper distance. In fact, as shown in Figure 4, ligand **1b** shows Van der Waals interactions (pink dashed lines) with different amino acids with respect to the active ligands, in particular γM81, γY141, and αA161 and it does not engage any hydrogen bond interaction with γT142.

In low-affinity compounds (**19–21,** K_i range 243–570 nM), the only interactions with receptor protein are those of Van der Waals with αV203 and αY210 and a hydrogen bond interaction with αY160. The latter is an amino acid for which interactions only for low affinity and inactive compounds are evidenced. In Figure 5, binding pocket in compound **21** is depicted; the Van der Waals interaction (pink dashed line) and the hydrogen bond interaction (blue solid line) are also evidenced.

Conclusion

The aim of this work was to synthesize new derivatives with pyrazolo[1,5-a]quinazoline scaffold, as 5-deaza analogue of pyrazolo[5,1-c][1,2,4]benzotriazine, to evaluate their biological activity on $GABA_A$ receptor subtype. With disappointing, the 4- or 5-substitutions on this new system gave compounds lacking recognition of receptor protein and, then to rationalize these

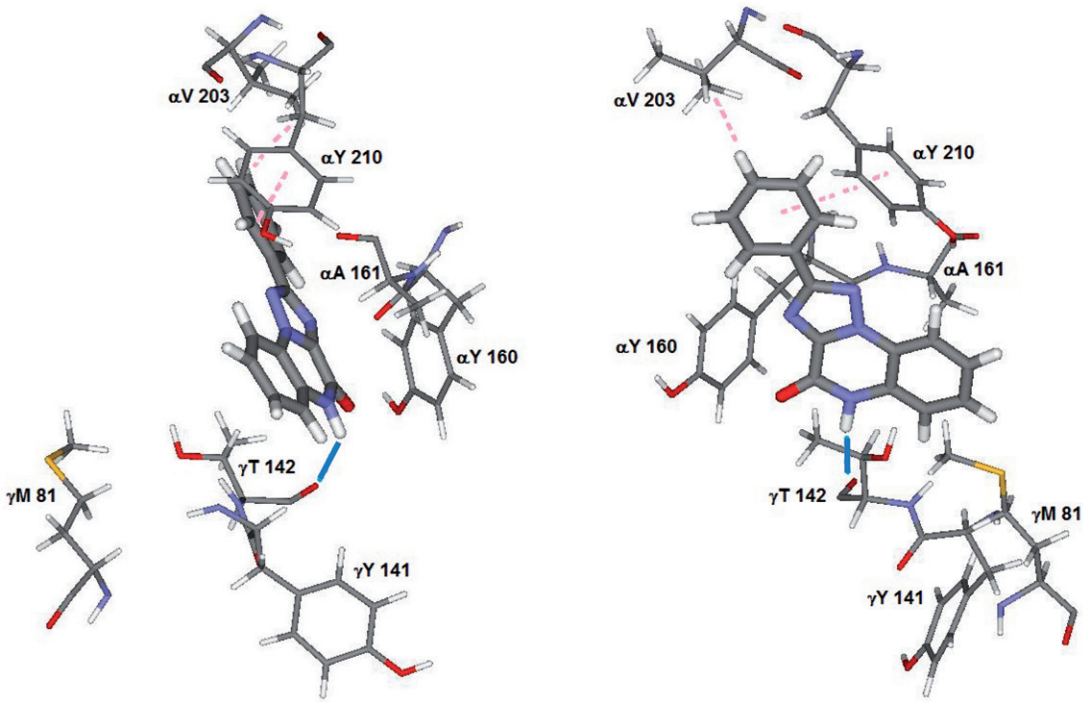

Figure 3. Interaction between affine compound **17** and receptor protein. Hydrogen bond interaction: blue solid line; Van der Waals interaction: pink dashed line.

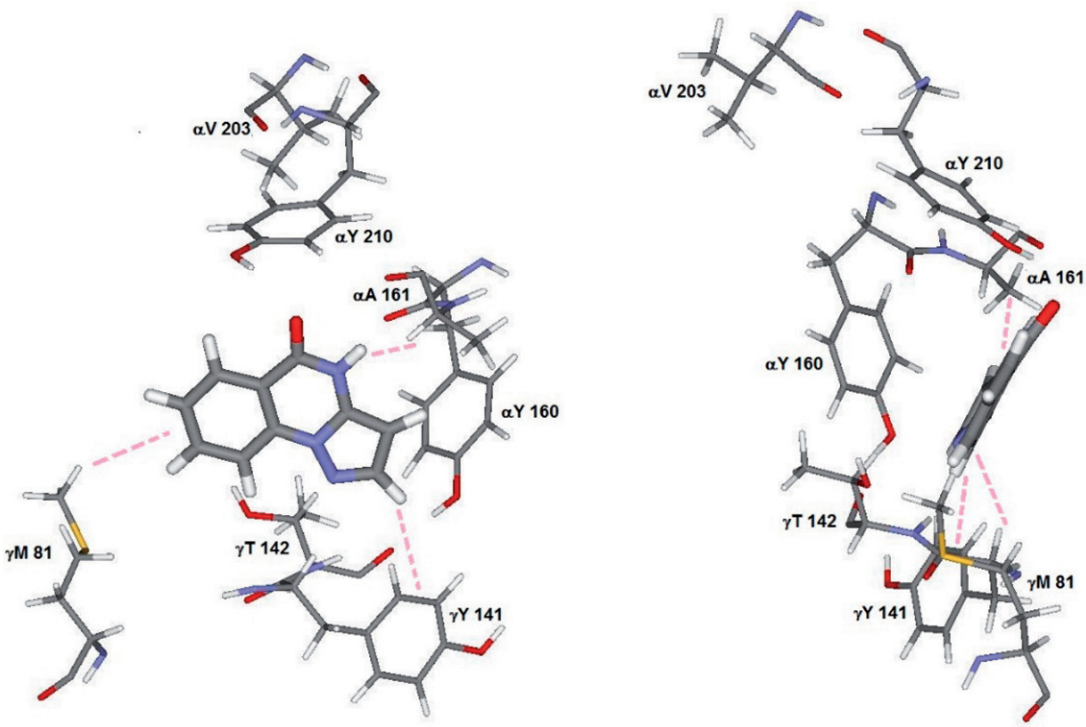

Figure 4. Interaction between affine compound **1b** and receptor protein. In particular, only Van der Waals interactions are evidenced, pink dashed line and they lack the hydrogen bond interactions.

results, a small library of the new and known compounds was properly chosen for a MDS. This study shows the importance of hydrogen bond interaction of ligand with γT142 of receptor protein, to enhance the binding affinity.

On the contrary, the unsaturation between 4 and 5 positions with achievement of the aromatization of the system was a necessary modification for binding affinity: in fact, compound **15** shows receptor recognition in nanomolar range. Based on these findings, further studies are in progress to investigate the pyrazolo[1,5-a]quinazoline system with suitable substituents in position 3 and/or 8, positions in the 5-azaanalogue system (pyrazolobenzotriazine) are proved to be compelling.

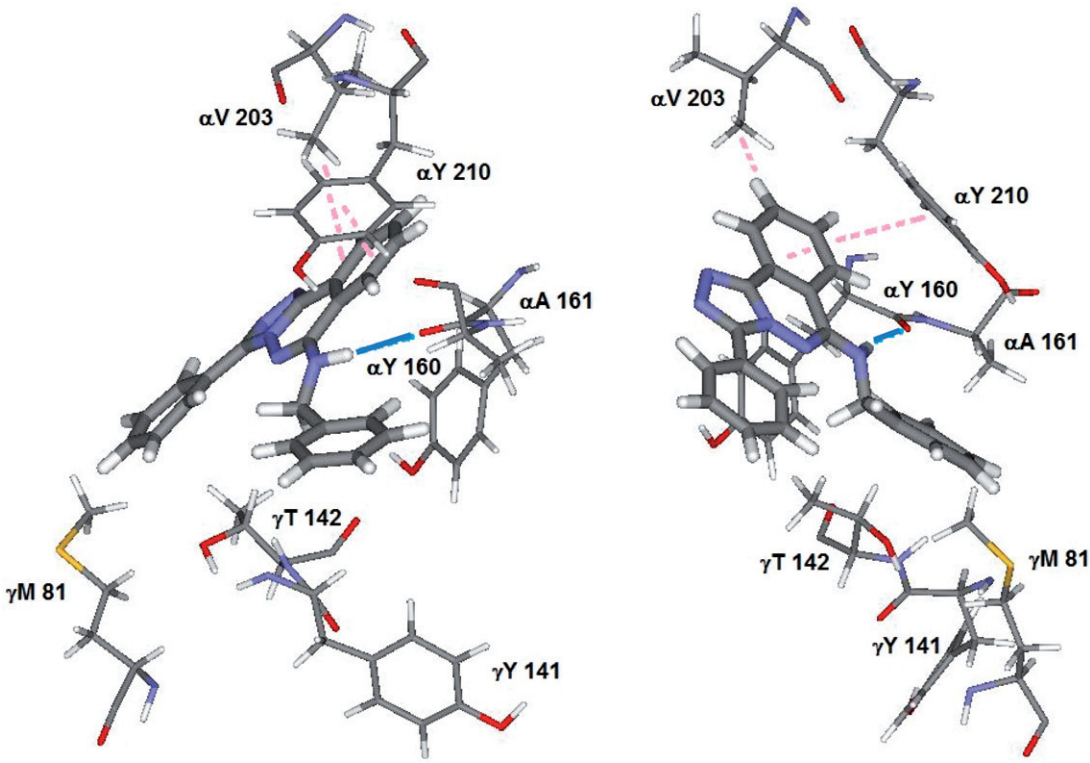

Figure 5. Interaction between affine compound **21** and receptor protein. In particular, Van der Waals interactions, pink dashed line, and the hydrogen bond interaction with αY160 are evidenced.

Declaration of interest

The authors report no conflicts of interest. The authors alone are responsible for the content and writing of this article.

References

1. Guerrini G, Ciciani G, Costanzo A, et al. Synthesis of novel cognition enhancer with pyrazolo[5,1-c][1,2,4]benzotriazine core acting at c-aminobutyric acid type A (GABA A) receptor. Bioorg Med Chem 2013;21:2186–98.
2. Guerrini G, Ciciani G, Bruni F, et al. Development of ligands at γ-aminobutyrric acid type A (GABAA) receptor subtype as new agents for pain relief. Bioorg Med Chem 2011;19:7441–52.
3. Guerrini G, Ciciani G, Bruni F, et al. New 3-,8-disubstituted pyrazolo[5,1-c][1,2,4]benzotriazines useful for studying the interaction with the HBp-3 area (hydrogen bond point area) in the benzodiazepine site on the γ-aminobutyric acid type A (GABAA) receptor. Bioorg Med Chem 2011;19:3074–85.
4. Wenthur CJ, Morrison RD, Daniels JS, et al. Synthesis and SAR of substituted pyrazolo[1,5-a]quinazolines as dual mGlu(2)/mGlu(3) NAMs. Bioorg Med Chem Lett 2014;24:2693–8.
5. Taliani S, Pugliesi I, Barresi E, et al. Phenylpyrazolo[1,5-a]quinazolin-5(4H)-one: a suitable scaffold for the development of noncamptothecin topoisomerase I (Top1) inhibitors. J Med Chem 2013;56:7458–62.
6. Colotta V, Catarzi D, Varano F, et al. Synthesis and binding activity of some pyrazolo[1,5-c]quinazolines as tools to verify an optional binding site of a benzodiazepine receptor ligand. J Med Chem 1996; 39:2915–21.
7. Catarzi D, Cecchi L, Colotta V, et al. Tricyclic heteroaromatic systems 1,2,4-triazolo[1,5-a]quinaxolines: synthesis and benzodiazepine receptor activity. Farm 1993;48:1065–78.
8. Bertelli L. Substituted 1,2,3-triazolo[1,5-a]quinazolines: synthesis and binding to benzodiazepine and adenosine receptors. Eur J Med Chem 2000;35:333–41.
9. Nilsson J, Gidlöf R, Nielsen EØ, et al. Triazoloquinazolinediones as novel high affinity ligands for the benzodiazepine site of GABA(A) receptors. Bioorg Med Chem 2011;19:111–21.
10. Costanzo A, Guerrini G, Ciciani G, et al. Benzodiazepine receptor ligands. 4: synthesis and pharmacological evaluation of 3-heteroaryl-8-chloropyrazolo[5,1-c][1,2,4]benzotriazine 5-oxides. J Med Chem 1999;42:2218–26.
11. Morris GM, Huey R, Lindstrom W, et al. AutoDock4 and AutoDockTools4: automated docking with selective receptor flexibility. J Comput Chem 2009;30:2785–91.
12. Jakalian A, Jack DB, Bayly CI. Fast, efficient generation of high-quality atomic charges. AM1-BCC model: II. Parameterization and validation. J Comput Chem 2002;23:1623–41.
13. Wang J, Wang W, Kollman PA, Case DA. Automatic atom type and bond type perception in molecular mechanical calculations. J Mol Graph Model 2006;25:247–60.
14. Case DA, Darden TA, Cheatham III TE, et al. AMBER 9. San Francisco, CA: University of California; 2006.
15. Wang J, Wolf RM, Caldewell JW, et al. Development and testing of a general Amber force field. J Comput Chem 2004;25:56531.
16. Jorgensen WL, Chandrasekhar J, Madura JD, et al. Comparison of simple potential functions for simulating liquid water. J Chem Phys 1983;79:926–35.
17. Darden T, York D, Pedersen L. Particle mesh Ewald: an *N*·log(*N*) method for Ewald sums in large systems. J Chem Phys 1993;98: 10089–93.
18. Ryckaert JP, Ciccotti G, Berendsen JC. Numerical integration of the Cartesian equations of motion of a system with constraints: molecular dynamics of *n*-alkanes. J Comput Phys 1977;23:327–41.
19. Connolly ML. Solvent-accessible surfaces of proteins and nucleic acids. Science 1983;221:709–13.
20. Costanzo A, Guerrini G, Bruni F, Selleri S. Reactivity of 1-(2-nitrophenyl)5-aminopyrazoles under basic conditions and synthesis of new 3-,7-, and 8-substituted pyrazolo[5,1-c][1,2,4]benzotriazine 5-oxides, as benzodiazepine receptor ligands. J Heterocycl Chem 1994;31:1369–76.
21. Alexander EJ. 4,5-Dihydro-5-oxopyrazolo[1,5-a]quinazoline-3-carboxylic acid derivatives. US1978/4105766 A1; 1978.

22. Mayer S, Schann S. Substituted pyrazoloquinazolinones and pyrroloquinazolinones as allosteric modulators of group II metabotropic glutamate receptors. WO 2013/174822 A1; 2013.
23. Peet PN. An unexpected aminolysis in the synthesis of 5-substituted 3-(1H-tetrazol-5-yl)pyrazolo[1,5-a]quinazolines. J Heterocycl Chem 1989;26:713–16.
24. Penning TD, Thomas SA, Hajduk PJ, et al. Potent PARP inhibitors. US2012/8183250 B2; 2012.
25. Lee NK, Lee JW, Lee S, et al. Quinazoline derivatives for the treatment and prevention of diabetes and obesity. 2006 WO2006071095A1. WO2006/071095, 2006.
26. Haddach M, La Jolla FP. Tricyclic compounds and pharmaceutical uses thereof. US2001/0065712 A1; 2001.
27. Ong CW, Liu M-C, Lee K-D, Chang KW, et al. Synthesis of bisquinoline–pyrrole oligoamide as G-quadruplex binding ligand. Tetrahedron 2012;68:5453–7.
28. Catarzi D, Cecchi L, Colotta V, et al. Reaction of 1-aminophtalazines with alpha-halocarbonyl compounds: imidazo[2,1-a]phtalazines and their benzodiazepine receptor activities. Il Farmaco 1993; 48:447–57.
29. Tarzia G, Occelli E, Toja E, et al. 6-(Alkylamino)-3-aryl-1,2,4-triazolo[3,4-a]phthalazines. A new class of benzodiazepine receptor ligands. J Med Chem 1988;31:1115–23.
30. O'Mara M, Cromer B, Parker M, Chung S-H. Homology model of the GABAA receptor examined using Brownian dynamics. Biophys J 2005;88:3286–99.

Supplementary material available online
Supplementary Table S1 and Figure S1.